Available online at www.sciencedirect.com
ScienceDirect
Physics Procedia 5 (2010) 473–481
Physics Procedia
www.elsevier.com/locate/procedia
LANE 2010

Temperature field measurement as quality assurance measure in case of laser material processing

Marius Jurca*, Hans-Jürgen Langer

MEL Mikroelektronik GmbH, Breslauerstr.2, 85386 Eching, Germany

Abstract

The paper presents the results of the development of a new real-time quality assurance sensor. The Temperature Field Sensor is capable to offer a more direct interpretation of the monitoring results in correlation with the processing results and settings. The sensor delivers a temperature map of the heat-affected zone independent from processing parameters like welding speed. Using fibre optics, the sensor head of the new monitoring system has a small size matching the requirements for integration even in case of 3D-applications. The simultaneous acquisition of the distance and of the surface emissivity for each measuring point enables the system to monitor also low-emissivity materials like Aluminium. There is no limitation concerning the geometry of the joints to be monitored.

Keywords: Process Optimisation; Process Sensing & Control; Temperature Field Measurement; Distance Measurement

1. Introduction

The thermal joining and cutting processes have experienced a continuous grow in automation during the past two decades at least. Better lasers and a better understanding of the involved processes have enabled this grow. In the same time welding and cutting became difficult due to higher processing speeds, more demanding geometries requiring a higher flexibility, different materials, small budgets and less space for integration. These problems did not eliminate the zero-failure requirement.

* Corresponding author. Tel.: +49 89-327-1500; fax: +49 89-319-2023.
E-mail address: m.jurca@melsensor.de.

1875-3892 © 2010 Published by Elsevier B.V. Open access under CC BY-NC-ND license.
doi:10.1016/j.phpro.2010.08.075

1.1. Monitoring or Controlling the Joining Process?

Most of the running industrial joining applications are using up to a certain extent monitoring equipment supposed to assure constant and good results. The market acceptance for monitoring systems is at least in Germany relatively high. There are even applications, which would not exist without sensors and customised monitoring technology. On the other hand, only a few standard applications are using closed-loop control in order to achieve optimum results and such controllers usually cover only single production aspects, but not the entire process (e.g. seam tracking).

It seams that there are two reasons for the limited number of closed-loop controlled applications:
i) technical reasons concerning the control stability and the limited applicability range of the used models, and
ii) unacceptable liabilities for the supplier of the control technology, supposed to cover the risks involved in an automated production line. The available sensor systems for welding applications are either standard sensors coming from other applications like geometry sensors, or are dedicated process sensors supposed to detect specifically a process parameter like laser power or arc current etc. Combinations of geometry and process sensors are yet not known from the literature. In the same time numerous models and simulations have been developed, but usually they failed to prove the ability to deal with all existing processes, joint geometries, workpieces and settings of the unknown parameters. The output of most models is a joint geometry adapted temperature field development in time and 3D- space.

Based on these conclusions, the present paper proposes a new monitoring system as a combination of geometry and process sensors capable to deliver a temperature map of the heat affected zone corresponding to the mentioned process models. The implementation of such a measurement enables a more precise evaluation of existing models, which might lead to an important extension of their validity ranges and the possibility to develop closed-loop controlled processes.

2. Temperature Field Sensor (TFS)

The Temperature Field Sensor consists of a variable number of single non- contact surface temperature acquiring sensors mounted in a dedicated fixture to the joint geometry of concern. Thus the temperature field measurement covers the heat affected zone (HAZ) across and along the weld bead behind the welding pool, so that the simultaneous measurement of all single pyrometers offers a moment temperature map of the HAZ (see Fig. 1).

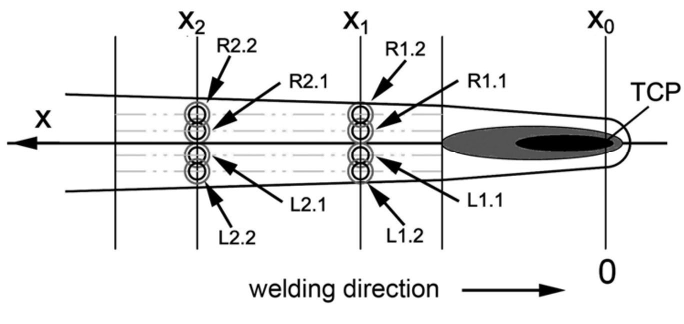

Fig. 1. Typical placement of the temperature spot sensors (Ra,b / La,b correspond to the location of the “RIGHT” resp. “LEFT” spot sensors)

A single temperature spot sensor acquires the irradiance of the pointed surface. The non-contact temperature measurement is governed by the Planck’s radiation law. After reshaping the relations, we obtain for the measured irradiance in case of a black body (see Fig. 2):

$$E_\lambda = \frac{r_S^2}{d^2} \cdot \cos\theta_S \cdot \int_{\lambda_1}^{\lambda_2} \varepsilon(\lambda,T) \cdot M_\lambda(\lambda,T)\, d\lambda \tag{1}$$

where r_S = radius emitting spot, d = measuring distance, θ_S = measuring angle, $\varepsilon(\lambda,T)$ = emissivity and

$$M_\lambda(\lambda,T) = \frac{c_1}{\lambda^5}\cdot\left(\exp\frac{c_2}{\lambda T}-1\right)^{-1} \quad (2)$$

with $c_1 = 2hc^2$ *and* $c_2 = hc/k$

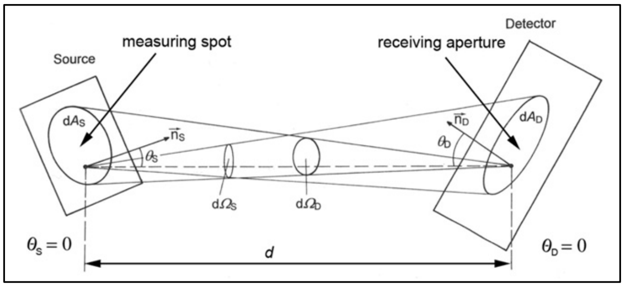

Fig. 2. Geometrical set up as reference for the formulas *(1)* and *(2)*

The relation *(1)* reveals the main problems concerning the non-contact temperature measurement:

- $E \sim d^{-2}$ the square law dependence from the measuring distance,
- $E \sim \cos\theta_S$ dependence from the measuring angle, in our case $\theta_S = 0$, thus $\cos\theta_S = 1$,
- $E \sim \varepsilon$ dependence from material, from surface finishing, from measuring wavelength and from temperature,
- $E \sim \lambda$ dependence from the acquisition wavelength band (here λ_1=1200nm, λ_2=1800nm).

For typical welding applications, the measuring distance can usually be kept constant within several 100µm, but still remains important due to the square law. The most critical factor is the unknown emissivity, because it strongly depends on the temperature, material sort and surface finishing for the temperature ranges of concern. Especially in case of Aluminium at room temperature the emissivity can vary between 0.02 and 02, which means that it is almost impossible to measure the irradiance.

2.1. Single spot temperature, emissivity and distance measurement

This paper proposes a new non-contact temperature sensor, which actively measures simultaneously the irradiance, the emissivity [1-6] and the distance in the same spot on the surface of interest. Due to the reduced space requirements in the working area, the sensor was supposed to be as simple and as small as possible. Thus it consists only of optical fibre bundles.

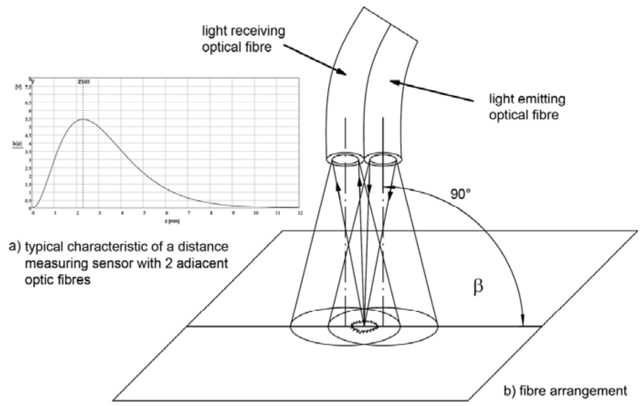

Fig. 3. Sketch of the distance measuring principle: a) typical shape of the distance characteristic, b) fibre arrangement

Figure 3 shows the principle of a distance measurement fibre sensor with adjacent fibres. The distance characteristic depends mainly on the emitting light power and on the reflectivity of the target surface, since the measuring angle $\theta_S = 0$. We eliminated the unknown reflectivity using the fact that the numerical aperture of a step index fibre depends on the wavelength. Thus emitting alternatively $\lambda_3 = 1550$ nm and $\lambda_4 = 658$ nm and measuring the reflected power two similar distance curves can be obtained, which are slightly shifted in z-position (see Fig. 4).

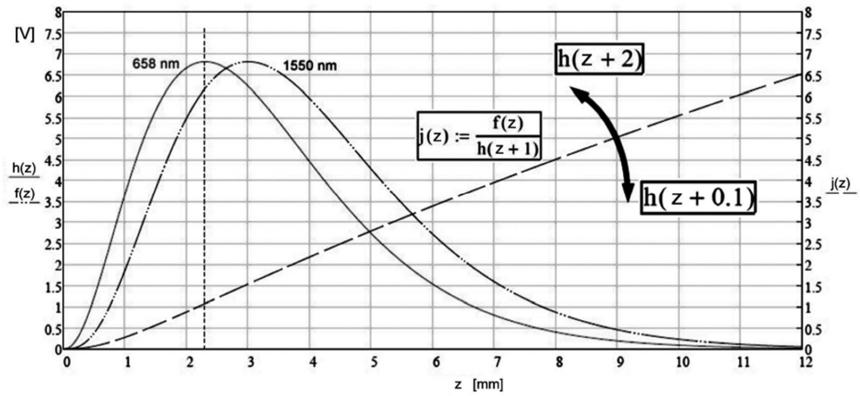

Fig. 4. Distance measuring curves at 658 nm and 1550 nm; j(z) corresponds to the ratio f(z)/ h(z)

Building the ratio of the two measurements the unknown reflectivity can be eliminated and the resulting distance characteristic can be linearised (see Fig. 4). The curves in Fig. 4 are interpolated measured data. The coordinate shift for the denominator function (z + 1) of the resulting j(z) has been found experimentally. Lower shifts generate a “saturation” – like curve and larger values an “exponential”- curve. The measuring range of d can be tailored according to the application needs, because it is dependent from the fibre-NA and the distance between two adjacent fibres. Thus the usable range is 3 mm up to 12 mm.

In case of “normal” surfaces the described distance measurement method would provide also the value of the reflectivity $r(\lambda, T)$. Under thermal equilibrium conditions the emissivity $\varepsilon(\lambda,T)$ can be calculated according to:

$$\varepsilon\left(\lambda,T\right)=1-r\left(\lambda,T\right) \qquad (3)$$

But the difference of the two wavelengths is too high for this and the measurement of the reflectivity would be insufficient precise. A higher precision for the reflectivity and indirectly for the emissivity measurement offer the measurement of the reflected light power having λ_3 = 1550 nm, because λ_3 is laying within the wavelength range for the irradiance measurement. In order to separate electronically this reflex measurement from the irradiance measurement, the emitted 1550 nm – light needs to be pulsed with an appropriate relatively high frequency. Doing so, only one InGaAs- photo detector is necessary for measuring either the irradiance (between λ_1=1200nm and λ_2=1800nm) and the reflected 1550 nm - light. For the reflectivity measurement the sensor needs a precise calibration on a perfect mirror placed at the nominal measuring distance. On this mirror the reflectivity measurement is calibrated to deliver *r(1550nm, 20°C)* = 1 (corresponding to 100% reflectivity and internally set to a signal level of 10V), thus any technical surface less reflective than the perfect calibration mirror delivers a reflectivity signal smaller than 10 V. Finally one sensor consists of three adjacent step index fibres sending light with λ_3 = 1550 nm and λ_4 = 658 nm and measuring selectively these wavelengths together with the irradiance measurement between λ_1 = 1200 nm and λ_2 = 1800 nm (see Fig. 5) [1, 4-6]. The experimental results show a negligible influence of the small tilting angles (up to ± 4°) of the measured surface with respect to the optical axis of the sensor.

For the sensor protection only pressurized inert gas (flow rate = approx. 1 l/min) and an appropriate mechanical holder are necessary. Thus the sensor is passive (no active components which could electromagnetically be influenced) and can be used in harsh environment and even under high vacuum conditions (of course, without purge gas).

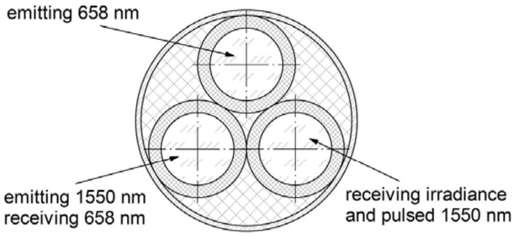

Fig. 5. Fibre bundle arrangement for a single spot temperature sensor

2.2. Implementation of the multi spot Temperature Field Sensor (TFS) and experimental results

A typical placement of the measuring spots in case of a symmetric butt joint is shown in Fig. 1. For optimum results the choice of the positions x_1 and x_2 (see Fig. 1) should generate temperature readings in the range of $T(x_1) \approx 2 \cdot T(x_2)$ for the nominal values of the welding process parameters. The lateral position of the measuring spots does not necessarily need to be symmetrical in respect to the weld, but should be symmetrical in respect with the measured temperature values. If possible T(R1.1/ R1.2) ≈ T(R2.1/ R2.2) ≈ 1.5 … 3.0, thus a maximum sensitivity for the evaluation of the current misalignment can be achieved. Each spot detector acquires $E_{SD}(T,d,r)$ where *r* and *d* are also measured and *K* is a instrument constant obtained by calibration:

$$E_{SD}\left(T,d,r\right) = K \cdot \frac{1-r}{d^2} \cdot f(T^4) \tag{4}$$

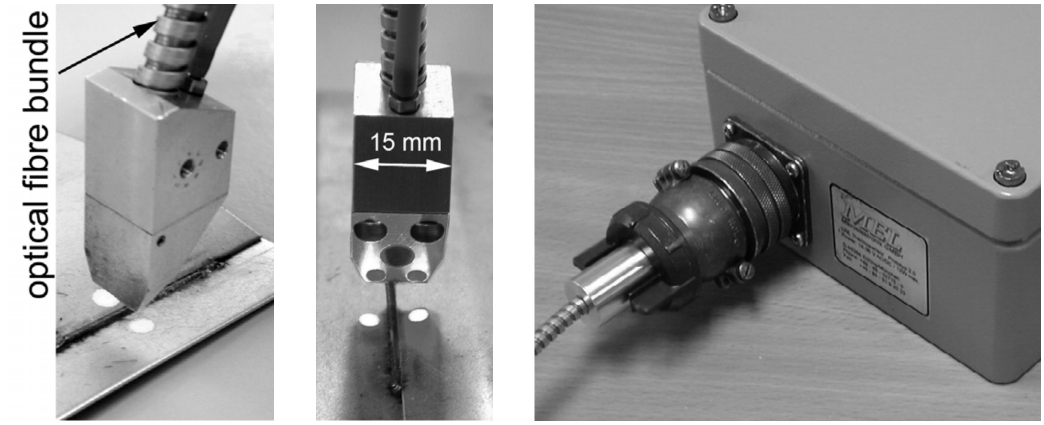

Fig. 6. Implementation of a two spot sensor unit a) and b), c) is the data acquisition unit

For special purposes the TFS can deliver the logarithms of the relation *(4)*, so that the output signal changes linearly with the temperature. In this case the lower limit of the temperature measuring range is about 320°C.

All signals of the spot sensors are acquired and processed simultaneously at a high frequency. Application dependent different arithmetic operations are calculated and monitored in real-time. Calculating the ratios according to the formulas *(5)* respectively *(6)* it is possible to detect a parallel offset in y-direction and in the same time an azimuth offset α.

$$\frac{R22+R12-L22-L12}{R22+R12+L22+L12} = y-OFFSET \tag{5}$$

$$\frac{R12-L12}{R12+L12} - \frac{R22-L22}{R22+L22} = \alpha-OFFSET \tag{6}$$

The advantage of these signals is related to the possibility to control with motorised axes the sensor position relative to the weld, enabling continuous monitoring even in case of 3D-curved welds.

Similar calculations along the weld bead deliver relationships capable to detect specifically and independently from each other a change of the laser power, of the focal distance or of the welding speed. Based on experiments e.g. defocusing the laser beam (in case of mild steel at 3.5kW and 1.5m/min) with 3 mm a reduced penetration depth is obtained. The same penetration reduction was obtained reducing the power by 20% at optimum focal position, but the temperature measured at x_1 is about 25% higher in case of defocusing than in the case of power reduction. The temperature measured at x_2 is similar in both cases. The temperature gradient between $T(x_1)$ and $T(x_2)$ is usually higher in case of power loss compared with the welding process under nominal conditions. For this evaluation the full-with-half-magnitude (FWHM) values of the temperature profile at the positions x_1 and x_2 are calculated and compared in realtime (see relations *7* to *10*).

$$\frac{R11+L11}{R11+R12+L11+L12} \approx T_{FWHM}(x_1) \tag{7}$$

$$\frac{R21+L21}{R21+R22+L21+L22} \approx T_{FWHM}(x_2) \tag{8}$$

Respectively:

$$\frac{R21+L21}{R11+L11} \approx grad\left[T_{MAX}(\Delta x)\right] \tag{9}$$

$$\frac{R21+R22+L21+L22}{R11+R12+L11+L12} \approx \frac{\int T(x_2)dy}{\int T(x_1)dy} \approx cooling-rate \quad (10)$$

The y- axis is laying perpendicular to the weld axis x and to the laser axis z. This simple experiment shows that typical ambiguities known from other temperature monitoring methods are avoided with the here presented new TFS.

In case of a typical laser welding process where for on-line monitoring purpose the weld bead temperature is monitored with a single spot pyrometer many of the possible process failures can be detected, due to signal changes, but several important ambiguities and unexpected signal signatures can be reported in case of real industrial applications. Some of the mentioned ambiguities can be described as follows:

There are three different possibilities to reduce the energy input per unit length: i) to reduce the laser power, ii) to defocus the beam or iii) to increase the welding speed. In all three cases the set-up can be optimised in order to obtain identical reductions of the weld penetration depth. The temperature signature is different in all three cases. Furthermore assuming that the temperature measuring spot has a realistic diameter of 5 mm, which can be considered very large compared with the diameter of the laser spot in TCP and that the distance to the TCP has a small value in the range of 20 mm, a set-up can be found (e.g. mild steel welding) where the temperature reading is higher despite the reduction of the energy input per unit length obtained by defocusing the beam. The explanation is simple: In case of defocusing, a larger part of the workpiece surface is heated and the maximum temperature of the weld bead would become a bit smaller. The heated area becomes larger and comparable with the area of the temperature measuring spot, thus the temperature reading (~ surface integral of the irradiance over the area of the measuring spot) becomes higher. It can easily be demonstrated that a higher welding speed might also lead to an increased temperature reading, due to the limited specific heat conductivity of the workpiece. In addition the temperature- and material- dependency of the emissivity factor as well as the sensor placement generate important limitations for using non-contact temperature measuring sensors in a welding environment. The new TFS eliminates or compensates most of the encountered problems.

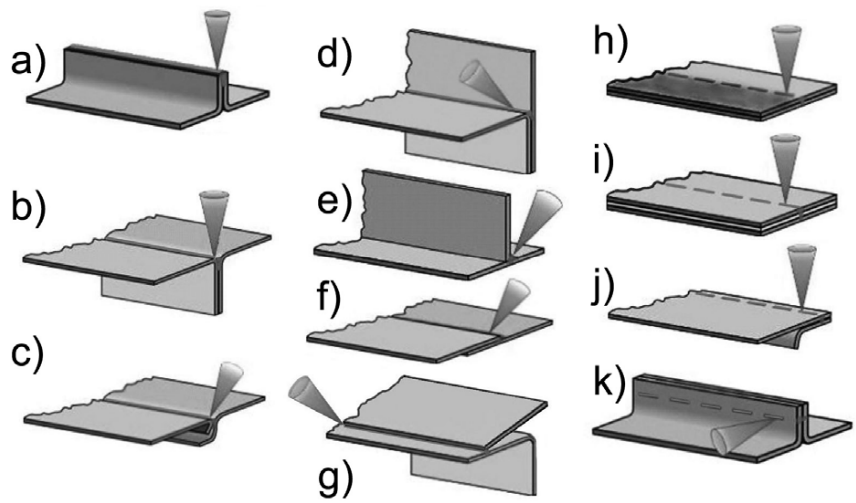

Fig. 7. Sketch of the most utilised weld geometries in case of thin sheets

In case of "T"-shaped or any other angled joint geometries (see Fig. 7) single spot temperature sensors are placed accordingly to measure onto each part to be welded. If necessary, the measurement can also take place additionally even underneath, if this side is accessible. The most powerful feature of the new monitoring method is the capability to acquire instantaneously the entire temperature map even in case of 3D-shaped joint geometries. Besides this feature and the resulting calculations of relations like *(5)* and *(6)* capable to be monitored in real-time, also the temperature evolution in time from the position x_1 can be followed at the position x_2 for the given speed of the process.

It is almost trivial the fact that misalignment with respect to the joint moves the weld into one of the parts to be welded and generates an important temperature difference between the left- and the right-side spot sensors. Fig. 8 shows a test sample of an overlap weld with filler wire according to Fig. 7 f). Here a progressive gap was prepared at the end of the weld. The corresponding signals from the lower part respectively from the upper part are shown in the Figures 9 a) and b).

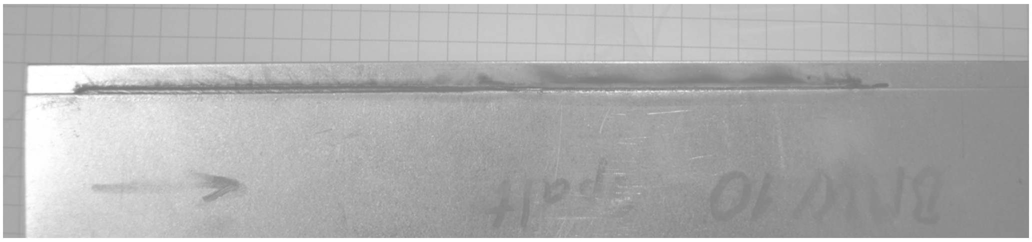

Fig. 8. Picture of a test sample according to the joint geometry from Fig. 7 f)

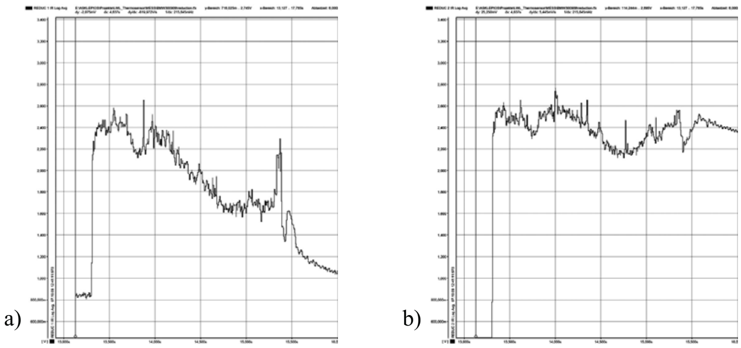

Fig. 9. Temperature signals on the lower part a) respectively from the upper part b) of the weld from Fig. 8

Despite the fact that both sides were hit by the laser and show a weld bead (also the weld root is visible) due to the linear gap between the sheets the molten metal of the filler wire moved inside the gap due to the gap capillarity. Figure 9 a) shows the corresponding drift of the temperature while Fig. 9 b) shows almost no change.

3. Outlook

The new Temperature Field Sensor (TFS) is a flexible and precise instrument capable to cover most of the requirements for quality assurance and monitoring purposes in all industrial beam or arc welding or other thermal treatment processes.

Due to the measurement of the emissivity of the workpiece surface of concern, the TFS can also be used to monitor Aluminium welding or brazing processes where the temperature of the specular surfaces cannot be acquired with simple pyrometers. The TFS is perfectly suited for the measurement within the temperature range which governs the transition from conduction to key-hole welding, because here the emissivity changes drastically with the temperature. The detailed temperature data offer a better chance for understanding the achieved metallic composition and the related hardness profiles.

The small size of the sensor head enables an easy adaptation of the TFS to any known application in this field. Especially due to its small size and capability to work under harsh environments and strong electromagnetic fields the Temperature Field Sensor can be integrated in hybrid welding systems. Based on TFS-measurements existing numerical models can be verified and improved. This can serve as background for a feedback-controlled process.

References

[1] C. Urs: Modellierung und praktische Anwendung einer neuen berührungslosen Temperaturmeßmethode, Diplom Thesis, University Babes-Bolyai, Cluj-Napoca, 2006

[2] M. Jurca: Temperaturmessen, schnelles Erfassen thermischer Vorgänge, Berührungslose Meßtechnik/ Sonderheft aus der Reihe „Praxis-Profiline, Vogel Verlag, ISBN 3-9259-1941-2, 2006

[3] M. Jurca, C. Urs: Telezentrischer Temperaturfeldscanner in der Qualitätssicherung, In: M. Zäh, G. Reinhart (Ed.): Inovation im Werkzeug- und Formenbau/ 3D-erfahrungsforum, Mai 30.-31.2007, München, Germany, 13.1 – 13.9

[4] M. Jurca, C. Urs: Telecentric Temperature Field Scanner for Quality Assurance, In: M. Geiger, A. Otto, M. Schmidt (Ed): Proc. of the 5th Int. Conf. LANE2007, Sept. 25.-28.2007, Erlangen, Germany, Meisenbach-Verlag, Bamberg (2007), Vol. 2, 993-1000

[5] M. Jurca, Non-contact measurement of the temperature profile of a surface, along a line, uses a rotating and transparent polygon scanner to pass emitted and/or reflected light from the surface to a focusing lens, Patent DE 102004053659 (2004)

[6] M. Jurca, Object surface's geometrical property detecting method, involves injecting light of light source in path of rays and detecting geometrical elevation profile of object by spectral and intensity moderate evaluation of rear reflex of source, Patent DE 102004053660 (2004)